Library Progress International *Print version ISSN 0970 1052*
Vol.44 No.3, Jul-Dec 2024: P.2329-2342 *Online version ISSN 2320 317X*

Original Article *Available online at www.bpasjournals.com*

Manufacturing and Controlling Robotic Arm Through Machine Learning via Electromyography Signal

Natiq A. Omran[1]*, Muhammed A. Al-Sattar[2] and Mithaq N. Raheema[3]

[1]Department of Biomedical Engineering, College of Engineering, Al-Nahrain University, Baghdad, Iraq
Department of Biomedical Engineering, College of Engineering, Warith Al-Anbiyaa, Karbala, Iraq
[2]Department of Systems Engineering, College of Mechanical Engineering, Al-Nahrain University, Baghdad, Iraq
[3]Department of Mechanical Engineering, College of Engineering, Karbala University, Karbala, Iraq
*Emai: natikaziz81@gmail.com
st.natiq.a.omran@ced.nahrainuniv.edu.iraq[1], M1976sjnr@gmail.com[2]and methaq.n.rhiama@uokerbala.edu.iq[3]

How to cite this article: Natiq A. Omran, Muhammed A. Al-Sattar, Mithaq N. Raheema (2024). Manufacturing and Controlling Robotic Arm through Machine Learning Via Electromyography Signal. *Library Progress International,* 44(3), 2329-2342.

ABSTRACT

Industrial robotics has advanced significantly as a result of automation's quick progress, and its applications in biomedicine, particularly in rehabilitation technology are growing. The goal of this project is to design, construct, manufacture and test a low-cost, six-degree-of-freedom 3D-printed Thor robotic arm that is controlled by surface electromyography (sEMG) signals. These signals were gathered from nine healthy volunteers utilizing a wireless Myo motions armband, and they made it possible to distinguish between seven different hand gestures.

Because of its mechanical robustness, polylactic acid (PLA) was employed in 3D printing, which added to the Thor prototype's endurance and open-source nature. Two Arduino Mega controllers and Ramps interface boards improved the electronic system, and Marlin firmware and Arduino-based software were used to govern control. Workspace navigation was used to evaluate the system and install an extra stepper motor to increase torque at the base joint.

Support Vector Machines (SVM), K-Nearest Neighbors (K-NN), and Linear Discriminant Analysis (LDA) were the three classifiers used for gesture detection. With an accuracy of 95.04% for dominant hands and 83.41% for non-dominant hands, SVM demonstrated the best accuracy. Additionally, SVM achieved near-perfect accuracy in elbow flexion-extension identification (99.55% for dominant and 98.73% for non-dominant), while LDA and K-NN also shown strong performance.

I. INTRODUCTION

A robotic arm consists of a series of movable links connected by joints, forming a chain. One end, typically fixed to a base, supports a hand or end-effector at the other end, which can move freely in space. Robotic arms can perform repetitive tasks with far greater speed and precision than human operators [1].The growing demands for quality and productivity in industrial settings necessitate the use of advanced solutions. Computer-controlled robotic manipulators offer numerous benefits, including enhanced precision and flexibility in production processes and improved working conditions for human workers by taking over labor-intensive, hazardous, or repetitive tasks [2].

Industrial robots operate in a manner analogous to human arms, consisting of rigid links connected to a base. These links allow movement in six degrees of freedom, enabling the robotic arm to maneuver in various directions and perform complex tasks [3].Robotic arms are used for pick-and-place, manufacturing, and

assembly operations [4]. The industrial robotic arm is a product with high added value. However, advancements in 3D printing technology have made it possible to produce the necessary components for constructing a robotic arm at a reduced cost without compromising quality. This manufacturing process, which builds three-dimensional objects through layer-by-layer material deposition, offers a cost-effective solution [5]. The procedure is directed by drawings generated using computer-aided design (CAD) software, enabling precise manufacturing of specific parts as shown in figure (1). In the context of globalization, numerous open-source projects for 3D printing are available in virtual repositories. This method offers several advantages, including flexibility, cost reductions, and potential applications in academic settings [6].

Figure (1): Complete assembly Thor robotic arm components design CAD model

The majority of that research typically makes use of highly basic robotics, such as industrial robots or servo motors. There aren't many articles that describe the mechanical couplings, gears, and electronic drive systems of robotic systems in detail. Servo motors with low torque are typically used in robots with simpler structures [7].

Research on the application of robotic arms is constrained by the high costs and complexity of the required components. Currently, there is a strong interest in various control systems, particularly adaptive systems enhanced with artificial intelligence [8]. The application of advanced robotic systems through additive manufacturing has the potential to revolutionize robotics by enabling the low-cost production of highly complex robots with professional-quality finishing. A notable finding of this study is the use of stepper motors instead of servo motors [9]. As torque increases, servomotor costs grow exponentially. Stepper motors are also incredibly precise, but they are significantly less expensive and have very easy controls [10].In the field of robotics, there is currently a clear division between research conducted in university and industry. Although the bulk of products have a simplified control, robotic arms are found in the industry with high cost and robustness. Mathematical modeling and complex control systems are often used in the academy to create low-cost, low-precision mechanical constructions [11].

Machine learning is one application of artificial intelligence. It is built on algorithms taught by data, which don't need to be explicitly coded in order to automatically learn to make predictions, improve over time, or act on data [12,13].

Three terms are combined to form the word electromyogram: myo, which is Greek for muscles, electro, which means related to electric activity, and gram, which means recording. Electromyography (EMG) is a medical diagnostic procedure that measures and examines the electrical signals produced by the skeletal muscles. An electromyography device, which produces an electromyogram, is used to do this [14]. Upon traversing several tissues, the EMG signal accumulates with overlapped noise. In addition to that, The EMG sensor collects signals. simultaneously from many motor units, particularly if they're close to the skin's surface, this can cause

different signals to interact. In biomedical engineering, the ability to detect EMG signals using innovative and efficient methods is gradually becoming essential. Clinical diagnostics and biological applications heavily depend on the analysis of EMG data. The definition of the field of motor disability rehabilitation and management is a major area of application. To classify EMG signal analysis and support the recommended actions, it is crucial to conduct an inquiry [15].

In many situations, the detection of sEMG signals is helpful and enhances fundamental techniques. Applications including biomedical engineering [16], robotic arms, and automation systems for controlling [17,18] are growing more and more in demand. The parameters of the electrodes and how they relate to the skin of the forearm or shoulder determine the measurements and accurate representations of the surface electromyography (sEMG) signals.

Control systems that use myoelectric control fall into two categories: those that recognize patterns and those that don't. Occurrence analysis, proportionate level control, and threshold level control are components of the non-pattern recognition control. Their degrees of freedom are limited, but they are all easy to employ in a real system [19].

In the past, myoelectric control algorithms and EMG signals have required expensive devices. Low-cost technologies (such as sensors, actuators, and controllers) and hardware support for simulation software programs like MATLAB have made myoelectric control studies more widely available [20]. It is important to choose the window length correctly in real time so that an appropriate delay may be achieved. Increased window length would result in higher classification accuracy but a slower classifier [21]. Time-domain (TD), frequency-domain (FD), and time-frequency-domain (TFD) features can be extracted from sEMG data. [22]. The implementation of TD features extraction is simple and doesn't involve a lot of computing power. From the data, RMS, the ZC, the SSC, the MAV, WL, and AR are retrieved from TD characteristics; these features are infrequently connected to the amplitude and frequency that are the original sEMG signals. On the other hand, Power Spectral Density (PSD) is extensively used to extract FD features [23].

The classifier will use the previously supplied feature-class sets to recognize the intended movement. The classifiers are used to differentiate across various feature sets. A number of techniques, such as popular techniques like fuzzy logic (FL), artificial neural networks (ANN), K-NN, SVM, and LDA, are employed for the purpose of classification [24]. The inexpensive generic wearable, the Myo gesture armband with many channels and integrated noise reduction filters, is the main component of the current work-study. This project's primary objective is to move the Thor 3D Printed Open Source 6-Dof Robotic Arm in real-time by substituting the wireless Myo gesture armband for the cable electrodes required for the sEMG signal. The subject's hand movement will be more comfortable and liberated with this replacement. Furthermore, compared to other sEMG sensors, the Myo armband is typically less priced. This study aims to demonstrate the implementation of an industrial robotic arm based on the open-source Thor project, emphasizing its modeling, firmware, and open-source software. Changes were made to the electronic system by integrating two Arduino Mega systems with interface boards to control all actuators, along with software tailored for 3D printing. Modifications included enhancing torque at the base with an additional stepper motor at the first joint and installing new end-of-stroke sensors. Validation of the project involved operational testing of the robot. Challenges encountered and solutions devised were presented to suggest potential improvements. To reduce production costs and enhance durability, PLA material was substituted as planned for the project. This approach offers significant cost-effectiveness, particularly in resource-constrained settings such as research and educational institutions in developing countries. Consequently, this research is expected to contribute to advancements in robotics education and research.

Also focusing on the development and deployment of a flexible prototyping robot for testing myoelectric control algorithms for rehabilitation engineering, utilizing a low-cost Arduino board and MATLAB programming. A range of EMG-based algorithms can be implemented on the platform in order to: (1) Process signals; (2) Extract features; (3) Identify patterns; (4) Combine sensor data; and (5) Perform real-time myoelectric control. By using pattern recognition-based myoelectric control to categorize seven human actions at the upper limb level and to operate a robotic upper extremity, the study platform was assessed. Subsequently, a real-time program was implemented to simulate the user's movements on the robotic arm.

In this article, in section II, the materials and methods used in the project are presented. Then, in section III, the obtained results are presented, as well as their discussion. The final conclusions are found in section IV. Section V concludes with recommendations for further research.

II. MATERIALS AND METHODS

The open-source design developed by Muro (2019) for a printable Thor robotic arm was utilized in this paper we to guide and conduct the investigation. With six degrees of freedom and a rotating wrist, this robotic arm is comparable to the majority of the current robot manipulators available on the market today, which feature rotating joints at every joint. [25]

More accurate and inexpensive movement transmission is made possible by the seven Nema17 stepper motors (original design) with different parameters that regulate its joints' movement. Figure (2) displays both the developed prototype and the adopted model. For more torque, joints 2 and 3 were equipped with motors that had a 5:1 gearing. The last two joints (5 and 6) feature smaller stepper motors because it is not optimum to have too much weight in this section of the robot. As motor drivers, seven Pololus A4988 [25] were employed. GT2 belts and pulleys powered joints 3, 5, and 6.

According to the original project, all required drivers can be inserted into an electronic system made up of an Arduino Mega and an interface board. It was also mentioned that the robot may be controlled by using the Universal GCODE Sender and the GRBL firmware. This project made use of the same hardware used in RepRap open-source 3D printers. As shown in figure 3, the electronic system consisted of two Arduino Mega boards and two Ramps.

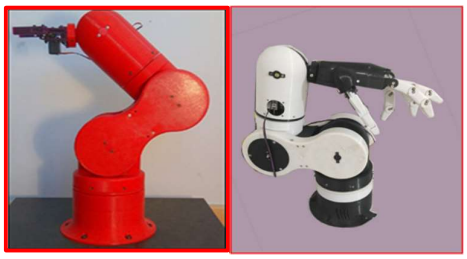

Figure 2: Thor robotic arm [25] on the left and prototype developed by the author on the right.

Characteristics	Nema 17	Nema 17 Without box	Nema 17 of reduction 5:1
Length (mm)	40	34	34
Phase Current (A)	0.4	0.4	0.4
Holding Torque (N.cm)	40	110	25.4
Phase angle (◦)	1.8	1.8	1.8
Mass (g)	240	500	280
Position (Together)	J1	J2, J3	J4, J5, J6

Table 1: specification of engines

Table (1) displays the specifications of the original engines used in each of the joints. The project model suggests using PLA plastic (polylactic acid) as the printing material.

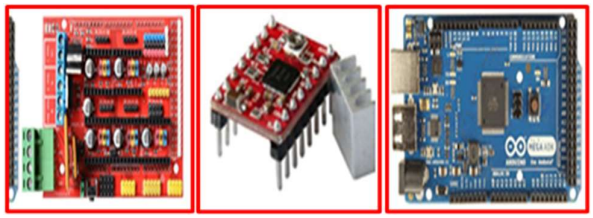

Figure 3: Ramps shield, Pololu A4988 driver and Arduino Mega board.

Figure (8) shows a block diagram of the myoelectric control-based platform. The target controller was determined to be the open-source Arduino MEGA2560 model. The mechanical structure was made of aluminum, and the segments were connected by articulating joints that allowed for rotation. The articulated robot has six degrees of freedom, allowing it to evaluate myoelectric control algorithms in real time and execute complex movements that are similar to those of a human arm.

Simulink has been offering hardware support packages for third-party products like Arduino since MATLAB version R2020b. It is necessary to obtain drivers from the Internet and choose the right product (in this case, an Arduino Mega). The model must then be configured to operate on the target, in this example an Arduino MEGA2560. One of Simulink's most useful features for Arduino hardware support is the real-time connection for model parameter adjustment.

III. RESULTS AND DISCUSSION

A. Development

First, the design of the components that were going to be printed out of the robot and their corresponding assemblies were studied using the free CAD program. Following the study, the project's starting point was completed, which involved printing 51 pieces without additive wrist and 68 pieces with it. In order to install the motors, belts, and optical sensors, a few instances of part reworking were required. Ultimately, the joints were partially assembled (figure 4). The additive wrist showed in figure (5).

Figure (4): components that are printed as well as incomplete joint assemblies.

Figure (5): The additive wrist for the original system

B. Modifications

It was discovered during testing using the prototype's whole assembly that the motor listed in joint 1's model does not have sufficient dynamic torque to move the structure. To move the same joint in the same rotational direction, a new motor was thus put on. Table VI displays more engine specifications.

c. Comparison

To qualify the developed prototype, physical properties were compared with those of industrial robotic arms that are currently on the market; the results are displayed in Table (2)[26].

Table (2): Comparison of Specifications of Industrial Robotic Arms

Model	Payload kg	mass	DOF	reach(mm)
WAM	3	25	7	3.5 m^3
RV-2A Mitsubishi	2	37	6	706
S1A10D Motoman	10	60	7	720
Am501C/5L Fanuce	5	29	6	892
TX40 Staubl	2	27	6	515
IRB120 ABB	3	25	6	700
S560 Adept Viper	2.5	28	6	653
KR5 R560 KUKA	5	28	6	650
RS03N Kawasaki	3	20	6	620
Prototype	0.75	6.1	6	427.5

Because of the sampled data, it is easy to see that the prototype and the other models differ significantly in material mass and payload.

The prototype has a mass that is roughly 5.75 times lower than the Am501C/5L Fanuce model and the TX40 Staubl model, respectively, however it is only 17% and 52% lighter in mass. In terms of degrees of freedom (DOF), most robots show a similar behavior. Table (3) provides more technical information on the prototype. It is possible to see the range of motion of the joints. The physical limitations caused by the model's design define the movement angle values of the prototype, which also make an effort to prevent internal wire twisting.

Characteristics Proto type Base Dimension (mm) Ø200 Height Dimension (mm) 635	
Joint name	Angle of Movement
Joint one	+180◦ to -180◦
Joint two	+90◦ to -90◦
Joint three	+135◦ to -135◦
Joint four	+180◦ to -180◦
Joint five	+90◦ to -90
Joint six	+180◦ to -180

Tabel (3): Specify Prototype Techniques

To illustrate a prototype's working space, it was A schematic figure is created (Fig. 6). Similar to the movement angles, the values given to the prototype are based on the model's physical constraints.

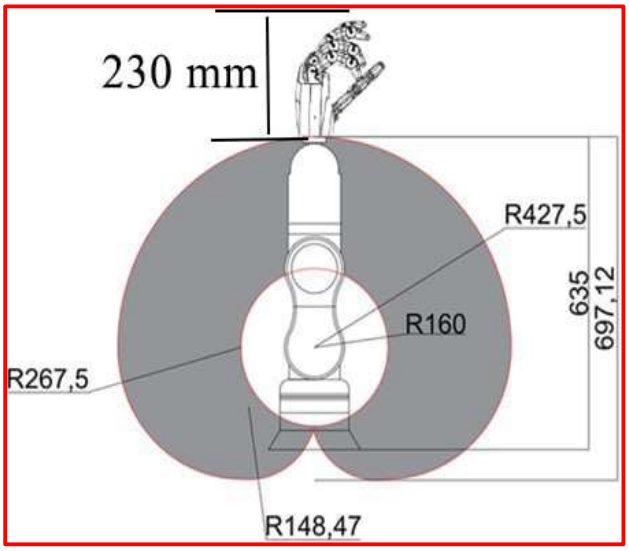

Figure (6): Work space prototype (measurements in millimeters)

D. Specifications of the Model

There are a few abnormalities with the approved model that could keep the prototype from moving as well as possible. Considerable friction is allowed to exist in joints 1 and 4 due to their bearing systems. Joint 1 has a totally PLA-printed bearing, while Joint 4 has airsoft balls for handling (Figure 7).

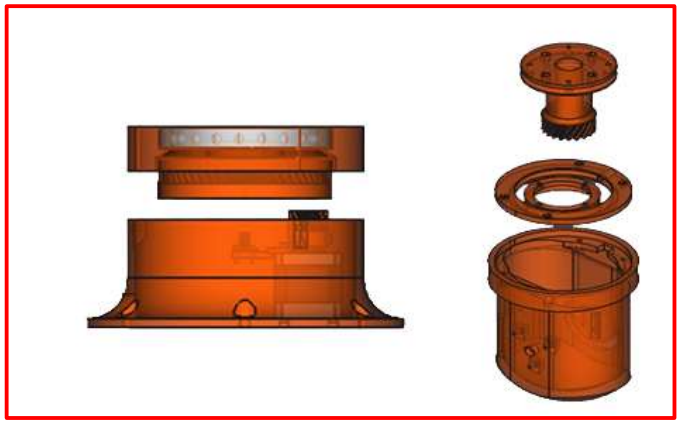

Figure (7): The corresponding bearing systems for joints 1 and 4 [25].

E. Expectations, Differentials, and Contributions

This project shows how an open design for an industrial robotic arm may be validated and put into practice, showcasing its efficacy and suggesting ways to improve functionality. Especially in scientific and educational settings, creativity is enhanced by recording the stages of development.

Moreover, the project is renowned for its cost-effectiveness, giving significant added value compared to standard industrial robotic arms. Given the frequently low resources available for education and research in emerging nations, this feature is especially important. Using PLA materials—which are readily accessible in developed countries—the effort has successfully cut expenses without sacrificing the model's fidelity.

It is therefore expected that the approach offered in this work will greatly aid robotics research and instruction, particularly in environments with limited resources.

Numerous investigations have classified characteristics obtained from the sEMG using various methods, such as support vector machines (SVM), fuzzy classifiers, hidden Markov models, multi-layer perceptron (MLP), Bayesian classifiers (BYN), and linear discriminant analysis (LDA) [27–32]. Three popular classifier algorithm types are used in this study: LDA, SVM, and K-NN. A statistics classifier called an LDA is used to identify which fresh observations fall into classes that are mutually exclusive. Comparable to the SVM method, The

LDA seeks to identify a hyperplane capable of classifying the data points into different groups [33].The graphic below shows a block diagram of the proposed myoelectric algorithm. A feature extraction method that complies with a set of temporal domain parameters is applied to every epoch (or data window) in order to extract data from sEMG.

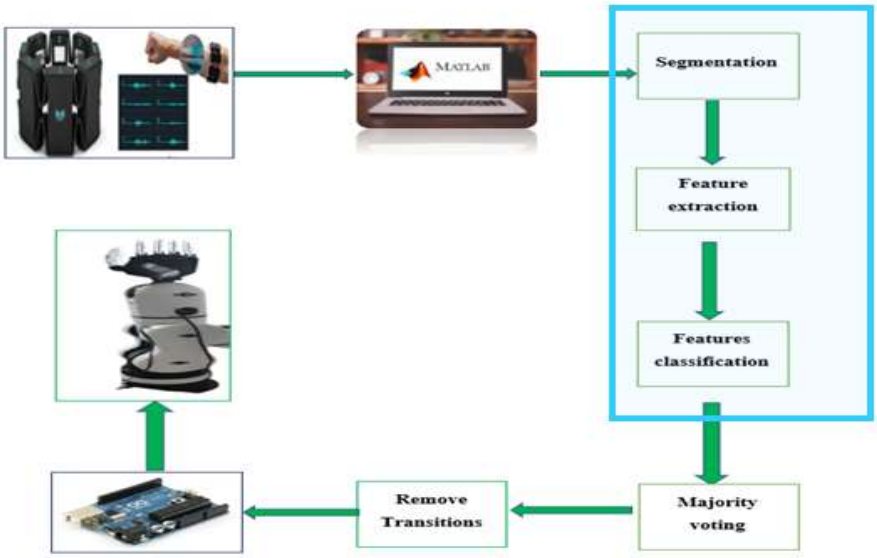

Figure (8): Block schematic of the myoelectric mechanism in practice

Eight files contained the seven gestures made by nine healthy participants. Each dataset has a 35-second duration, with each gesture starting with a hand gesture that is at rest and lasting five seconds. The complete dataset recording for each individual is 280 seconds long. A cross-validation technique was used to divide the dataset into training and testing sets. For cross-validation, the original dataset is randomly split into k equal-sized sub-datasets. One sub-dataset is retained as validation data for the model's testing, and the other sub-datasets are used as training sets. To do cross-validation, the recorded datasets were split up into eight smaller datasets. The data for each of the nine healthy study participants is shown in the table below.

Table (4): Information about the volunteered persons.

Number of Volunteer	Gender	Length (cm)	Weight (Kg)	Age (year)	Hand side
Volunteer 1	Male	186	102	35	Right and Left arm +forearm
Volunteer 2	Male	168	81	45	Right and Left arm +forearm
Volunteer 3	Female	164	99	36	Right and Left arm +forearm
Volunteer 4	Male	165	80	32	Right and Left arm +forearm
Volunteer 5	Male	176	96	42	Right and Left arm +forearm
Volunteer 6	Male	165	63	25	Right and Left arm +forearm
Volunteer 7	Male	158	66	33	Right and Left arm +forearm
Volunteer 8	Male	167	70	30	Right and Left arm +forearm
Volunteer 9	Male	166	75	48	Right and Left

					arm +forearm

Because of motion artifact, ambient noise, intrinsic noise in electronics equipment, and inherent instability of the sEMG signal, the obtained sEMG signals are usually noisy [34]. When utilizing the Myo gesture armband, the noise ratio in sEMG signals is essentially low and has no bearing on the sEMG data. The sEMG signals, which are typically very low in voltage between 0 and 2 mV, are enhanced by the Myo gesture armband [35].

For pattern recognition system, its parts can be summarized as below:

1. Segmentation

The window length of the signals had a substantial impact on the processing time and classification accuracy of sEMG signals in online mode. The information is greatly altered when the window length is very small, which results in low classification accuracy. It is therefore challenging to get important information from every window. To provide both high accuracy and short delay times, a trade-off between the two should be carefully considered. The window size in this study is adjusted from 30 to 120 milliseconds, with an increment of about half the window size. Figure (9) shows the result of increasing the window size applied on subject one dataset for SVM, LDA and KNN classifiers.

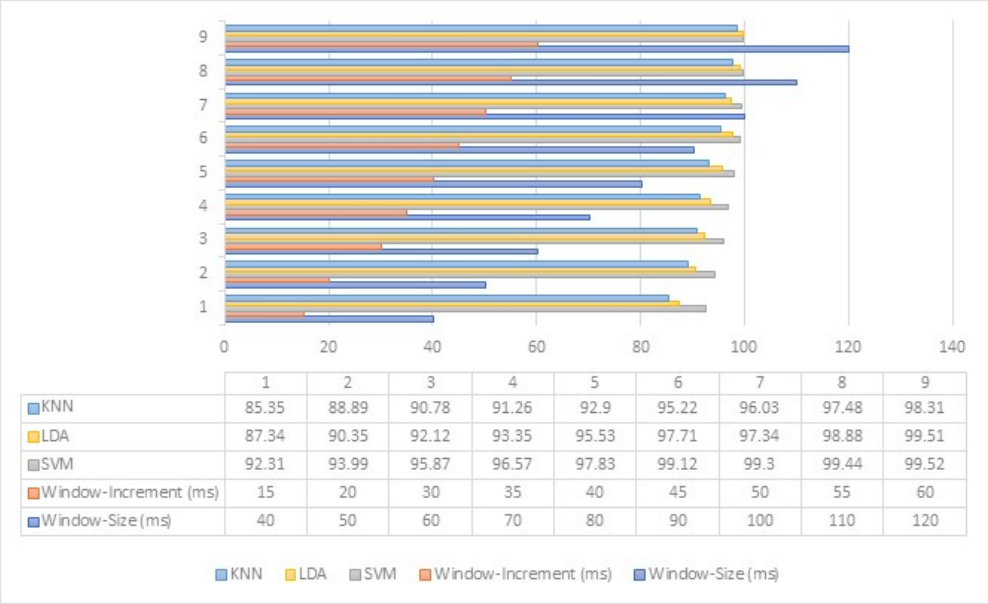

	1	2	3	4	5	6	7	8	9
KNN	85.35	88.89	90.78	91.26	92.9	95.22	96.03	97.48	98.31
LDA	87.34	90.35	92.12	93.35	95.53	97.71	97.34	98.88	99.51
SVM	92.31	93.99	95.87	96.57	97.83	99.12	99.3	99.44	99.52
Window-Increment (ms)	15	20	30	35	40	45	50	55	60
Window-Size (ms)	40	50	60	70	80	90	100	110	120

Figure (9): Effect of window size on system accuracy (%)

2. Feature Extraction

Certain features are chosen from each window of the sEMG signals after the signals have been separated into windows of the same size. These feature classes ensure high separation gesture accuracy. Features cannot be extracted from individual sEMG signal samples.The time domain characteristics in this work that were chosen for their simplicity of usage and little processing overhead are RMS, WL, AR (4), ZC, MAV, and SSC. A matrix of features is produced after these features are eliminated from each window for each channel of the sEMG signals. Both the number of rows in the matrix and the total number of features for every channel represent the total number of sEMG data windows. Results for SVM classifier as example shown.

No. of volunteers	RMS	WL	AR(4)	ZC	SSC	MAV	All Features
Volunteer 1	95.72	93.20	70.67	47.69	34.38	94.55	94.22
Volunteer 2	92.85	91.24	64.78	48.74	40.41	92.28	94.11
Volunteer 3	94.90	91.06	60.86	39.53	28.90	92.48	93.87
Volunteer 4	93.27	91.14	61.63	43.96	37.92	90.31	95.55
Volunteer 5	94.32	92.47	65.93	44.71	33.19	93.99	93.52

Volunteer 6	**92.95**	**90.50**	**54.22**	**40.24**	**30.79**	**93.48**	**93.65**
Volunteer 7	**91.93**	**89.97**	**63.85**	**42.48**	**34.79**	**95.01**	**95.86**
Volunteer 8	**93.78**	**90.89**	**61.89**	**40.91**	**30.76**	**90.28**	**94.32**
Volunteer 9	**93.08**	**91.07**	**61.94**	**41.09**	**31.87**	**92.68**	**92.65**
Average	**93.64**	**91.28**	**62.86**	**43.26**	**33.66**	**92.78**	**94.19**

Table (5): Results of TD features using SVM classifier show the system accuracy (%) crosses all subjects.

2.1 Time Domain (TD) features

The frequency and amplitude measurements are particularly helpful when interpreting the sEMG movement state [36]. Features related to amplitude, such as mean absolute value (MAV) and waveform length (WL), and features related to frequency, such as zero crossings (ZC) and slope sign changes (SSC), will be used to extract relevant information about frequency and amplitude from the temporal sEMG signals [37-38]. Thus, one of the various applications of TD that have emerged recently is the pattern detection of sEMG signals for the purpose of controlling upper limb prosthesis.

3. Feature's classification

In order to determine which classifier is more effective at generating higher system accuracy, the study carefully compares three classifiers: Support Vector Machine (SVM), Linear Discriminant Analysis (LDA), and K-Nearest Neighbors (K-NN) with K set to 7. Delving into a rich dataset, the analysis spans a spectrum of gestures across diverse channels, encompassing wrist movements (right, left, up, down), hand closure, hand opening, and rest hand positions. This exhaustive exploration is further enriched by the repetition of each gesture sequence eight times, while meticulously considering variations in transradial.

Number of volunteers	KNN Classifier		LDA Classifier		SVM Classifier	
	dominant	non	dominant	non	dominant	non
1ST volunteer	80.93	75.88	89.22	80.56	94.62	85.06
2ND volunteer	81.28	76.75	89.02	76.85	94.08	82.45
3RD volunteer	83.52	78.63	88.66	79.97	94.98	82.98
4TH volunteer	83.83	75.93	90.11	80.86	95.95	85.13
5TH volunteer	84.67	74.32	87.87	79.98	94.06	81.22
6TH volunteer	79.39	71.94	86.73	78.12	93.75	82.87
7TH volunteer	85.71	80.93	91.36	83.29	96.28	84.94
8TH volunteer	84.44	79.26	90.41	78.27	95.89	82.76
9TH volunteer	84.02	81.39	90.25	77.33	95.83	83.33
The average	80.03	77.22	89.29	79.47	95.04	83.41

Table (6): Classification accuracy of all transradial healthy volunteers for movement configurations of three degree of freedom (wrist flexion-extension, open-close hand, up-down hand with rest hand).

IV. CONCLUSION

This research demonstrates that, with access to a 3D printer, it is possible to create complex mechanical systems with acceptable finishing in resource-constrained environments. This approach helps bridge the gap in the quality of mechanical structures used in academic robotics. The proposed robot showcases the use of stepper motors instead of the more commonly employed servo motors for similar applications, achieving comparable torque and precision.

There are two ways the system can function: offline and online (real-time). The live mode is utilized to move the robotic arm in real time, while the offline mode is designed to calculate system accuracy and enhance system performance. MATLAB R2020 has been utilized to implement these two modes.

A. OFFLINE MODE

Every time the Myo gesture armband is used to record datasets, it must be worn in the same manner to guarantee that its sensors are positioned consistently. To avoid unpredictable readings, this problem must be considered when recording data. For this investigation, raw sEMG data from each channel during muscle contraction activity were collected using a Myo gesture armband. The Myo armband collects data, which is transferred to

the computer via Bluetooth for processing and analysis by MATLAB R2020. When the number of features (six features: RMS, MAV, SSC, ZC, WL, and AR with order=4) per window (segment) is multiplied by the number of Myo channels (eight channels), 48 features are obtained for each set for all channels.

B. ONLINE MODE

As indicated in table (1), the physical parts of the entire system in its real-time condition consist of the 6-DoF Thor robotic arm, Due Arduino microcontroller, Dell laptop, and Myo gesture armband.

To move the robotic arm like a human arm, data is collected by the Myo armband and sent to the computer via Bluetooth. A majority vote yields the classifier's most often predicted final motions. The robotic arm's reaction time to a human arm gesture plays a critical role in defining the system's performance.

Feature selection is essential to extracting information from sEMG signals since the classifier can distinguish between motions based on the retrieved information of these features. For six extracted features and eight channels for nine subjects in this trial, the average accuracy of the system was 94.19%, 91.11%, and 85.51% for SVM, LDA, and K-NN, respectively. The RMS feature had a substantial impact on the system's accuracy, while the ZC and SSC features had less of an impact, according to the offline findings displayed in table (5). Consequently, in order to save processing time and lower computational costs, these characteristics might be eliminated from the feature vector collection. As a result, the four features that determined online mode were AR, WL, RMS, and MAV. The wireless devices the system's adaptability and mobility were enhanced by the Myo gesture armband, which also processed the sEMG signals efficiently. It can be concluded from the trials that the SVM and LDA classifiers yielded the best results since they show how the size of the window and the arrangement of the sensors affect the accuracy of the system. However, reasonable results were obtained with the K-NN classifier. displays initial study findings for developing a cost-effective upper-limb robotic platform for the assistance and rehabilitation of patients suffering from motor impairments.

The platform will enable the development and evaluation of new myoelectric control algorithms for application in rehabilitation apparatus. As validation, a myoelectric control method was developed to decode seven upper-limb movements. Muscle activity signal classifiers (SVM, LDA, K-NN) are improved by optimizing feature selection, particularly when AR, WL, RMS, and MAV features are the emphasis. Processing of muscle activity signals is made simpler by using the Myo gesture armband. This study highlights the significance of window size and sensor placement, with SVM and LDA exhibiting the greatest results. Using myoelectric control algorithms, the research offers a low-cost robotic platform for upper body rehabilitation.

Finally, the project shows that the overall costs are far less than the average costs of industrial robot manipulators, which is in line with the study's goals of leveraging additive manufacturing. The project is especially attractive in resource-constrained environments because of its cost-effectiveness, which also draws attention to the significant disparity between project costs and the market value of industrial robotic arms

V. FEATURE WORK

This project's evolution can be used as a model for robotics, computer numerical control (CNC), and industrial processes research and teaching. Future work will investigate more algorithm features for real-time applications using the same approach.

REFERENCES

1) S. Balasubramanian, S. Guguloth, J. S. Mohammed, and S. Sujatha, “A self-aligning end-effector robot for individual joint training of the human arm,” Journal of Rehabilitation and Assistive Technologies Engineering, vol. 8, p. 205566832110198, Jan. 2021. doi:10.1177/20556.

2) L. Bo et al., “Hand gesture recognition using SEMG signals based on CNN,” 2021 40th Chinese Control Conference (CCC), Jul. 2021. doi:10.23919/ccc52363.2021.9549505.

3) S. Ma, K. Deng, Y. Lu, and X. Xu, “Error compensation method of industrial robots considering non-kinematic and weak rigid base errors,” Precision Engineering, vol. 82, pp. 304–315, Jul. 2023. doi: 10.1016/j.precisioneng.2023.04.007. S.

4) M. Mahil and A. Al-Durra, “Modeling analysis and simulation of 2-dof robotic manipulator,” in 2016 IEEE 59th International Midwest Symposium on Circuits and Systems (MWSCAS). IEEE, 2016, pp. 1–

4.

5) M. Z. Silva, T. Brito, J. L. Lima, and M. F. Silva, "Industrial robotic arm in machining process aimed to 3D objects reconstruction," 2021 22nd IEEE International Conference on Industrial Technology (ICIT), Mar. 2021. doi:10.1109/icit46573.2021.9453596.

6) R. Chang and M. F. Antwi-Afari, "Critical success factors for implementing 3D printing technology in construction projects: Academics and construction practitioners' perspectives," Construction Innovation, Aug. 2023. doi:10.1108/ci-04-2023-0060.

7) X. Yan, X. Yan, and K. Zhang, "An optimization algorithm for direct torque control of Industrial Robot Servo Motors," International journal of simulation: systems, science & technology, Jan. 2019. doi:10.5013/ijssst.a.19.05.09.

8) G. Chryssolouris, K. Alexopoulos, and Z. Arkouli, "Artificial Intelligence in manufacturing equipment, automation, and Robots," A Perspective on Artificial Intelligence in Manufacturing, pp. 41–78, 2023. doi:10.1007/978-3-031-21828-6_3.

9) M. Cheng et al., "Advanced Electrical Motors and control strategies for high-quality servo systems - a comprehensive review," Chinese Journal of Electrical Engineering, vol. 10, no. 1, pp. 63–85, Mar. 2024. doi:10.23919/cjee.2023.000048.

10) S. Ricci and V. Meacci, "Simple Torque Control Method for hybrid stepper motors implemented in FPGA," Electronics, vol. 7, no. 10, p. 242, Oct. 2018. doi:10.3390/electronics7100242.

11) P. Sutyasadi, "Control improvement of low-cost cast aluminum robotic arm using Arduino based computed torque control," Jurnal Ilmiah Teknik Elektro Komputer dan Informatika, vol. 8, no. 4, p. 650, Dec. 2022. doi:10.26555/jiteki. v8i4.24646.

12) An, Q.; Rahman, S.; Zhou, J.; Kang, J.J. A Comprehensive Review on Machine Learning in Healthcare Industry: Classification, Restrictions, Opportunities and Challenges. Sensors 2023, 23, 4178.

13) Boukhennoufa, I.; Zhai, X.; Utti, V.; Jackson, J.; McDonald-Maier, K.D. Wearable Sensors and Machine Learning in Post-Stroke Rehabilitation Assessment: A Systematic Review. Biomed. Signal Process. Control 2022, 71, 103197.

14) G. D. Clifford, "Blind source separation: principle & independent component analysis," in Biomedical signal and image processing, CRC Press LLC, 2008.

15) R. Chowdhury, M. Reaz, M. Ali, A. Bakar, K. Chellappan, and T. Chang, "Surface EMG Signal Processing and Classification Techniques," Sensors, vol. 13, no. 9, pp. 12431–12466, 2013.

16) Wang, N., Lao, K., Zhang, X., 2017. Design and Myoelectric Control Of An Anthropomorphic Prosthetic Hand. J. Bionic Eng. 14(1), 47–59.

17) Gonzalo, P., Holgado-Terriza Juan, A., 2015. Control of Home Devices Based on Hand Gestures, in: 2015 IEEE 5th International Conference on Consumer Electronics - Berlin (ICCE-Berlin). IEEE, Berlin, Germany, 510–514.

18) Pham, T.X.N., Hayashi, K., Becker-Asano, C., Lacher, S., Mizuuchi, I., 2017. Evaluating the Usability and Users' Acceptance of a Kitchen Assistant Robot in Household Environment in:2017 26th IEEE International Symposium on Robot and Human Interactive Communication (RO-MAN). IEEE, Lisbon, Portugal,987–992.

19) S. Tallam Puranam Raghu, D. MacIsaac, and E. Scheme, Decision-change informed rejection improves robustness in pattern recognition-based myoelectric control, 2023. doi:10.36227/techrxiv.22492711.

20) T. Kang, "The current status of EMG signals on kinematics needed for precise online myoelectric control and the development direction," E3S Web of Conferences, vol. 271, p. 01029, 2021. doi:10.1051/e3sconf/202127101029.

21) D. Blanco-Mora et al., "Finding the optimal time window for increased classification accuracy during motor imagery," Proceedings of the 14th International Joint Conference on Biomedical Engineering Systems and Technologies, 2021. doi:10.5220/0010316100002865 .

22) S. Karheily, A. Moukadem, J.-B. Courbot, and D. Abdeslam, "Time-frequency features for SEMG Signals Classification," Proceedings of the 13th International Joint Conference on Biomedical Engineering Systems and Technologies, 2020. doi:10.5220/0008971902440249 .

23) W. Li and M. Wang, "Event identification using extracted features from high-dimensional power system data," 2018 52nd Asilomar Conference on Signals, Systems, and Computers, 2018. doi:10.1109/acssc.2018.8645220.

24) Nazmi, N.; Rahman, M.A.; Yamamoto, S.-I.; Ahmad, S.; Zamzuri, H.; Mazlan, S. A Review of Classification Techniques of EMG Signals during Isotonic and Isometric Contractions. Sensors 2016, 16, 1304.

25) A. Muro. (2019) Opensource 3d printable robotic arm. [Online]. Available: http://github.com/AngelLM/Thor.

26) A. Kholil, E. A. Syaefudin, A. Juniar, M. K. Rohim, and S. T. Dwiyati, "Simulation of temperature distribution in 3D printing heated chamber on orientation and temperature variations with PLA material," Journal of Physics: Conference Series, vol. 2596, no. 1, p. 012007, Sep. 2023. doi:10.1088/1742-6596/2596/1/012007.

27) P. Angkoon, P. Pornchai, and P.L. Chusak, "Feature reduction and selection for EMG signal classification", Expert Systems with Applications, vol. 39, pp. 7420-7431, 2012.

28) M. Zecca, S. Micera, M.C. Carrozza, and P. Dario, "Control of multifunctional prosthetic and by processing the electromyographic signal", Critical Reviews in Biomedical Engineering, vol. 30, no. 4, pp. 459-485, 2002.

29) K. Englehart, B. Hudgins, P.A. Parker, and M. Stevenson, "Classification of the myoelectric signal using time-frequency based representations", Med. Eng. Phys., vol. 21, pp. 431-438, 1999.

30) K. Englehart, B. Hudgins, and P.A. Parker, "A wavelet-based continuous classification scheme for multifunction myoelectric control", IEEE Trans. Biomed. Eng., vol. 48, no. 3, pp. 302-310, 2001.

31) A.D.C. Chan, and K. Englehart, "Continuous myoelectric control for powered prostheses using hidden Markov models", IEEE Trans. Biomed. Eng., vol. 52, no. 1, pp. 121-124, 2005.

32) A.B. Ajiboye, and R.F. Weir, "A heuristic fuzzy logic approach to EMG pattern recognition for multifunctional prosthesis control", IEEE Trans. Neural Syst. Rehabil. Eng., vol. 13, no. 3, pp. 280-29, 2005.

33) J. Tehrani, B. Nasihatkon, K. Al-Qawasmi, M. R. Al-Mousa, and R. Boostani, "An efficient classifier: Kernel SVM-LDA," 2022 International Engineering Conference on Electrical, Energy, and Artificial Intelligence (EICEEAI), Nov. 2022. doi:10.1109/eiceeai56378.2022.10050472].

34) B. Zhang et al., "A noise-suppressing neural network approach for upper limb human-machine interactive control based on SEMG signals," Frontiers in Neurorobotics, vol. 16, Nov. 2022. doi:10.3389/fnbot.2022.1047325 .

35) U. Côté-Allard, G. Gagnon-Turcotte, F. Laviolette, and B. Gosselin, "A low-cost, wireless, 3-D-printed custom armband for SEMG hand gesture recognition," Sensors, vol. 19, no. 12, p. 2811, Jun. 2019. doi:10.3390/s19122811.

36) A basic machine learning method for identifying individual biological state and ecological context from movement data," MODSIM2023, 25th International Congress on Modelling and Simulation., Aug. 2023. doi: 10.36334/modsim.2023.schaerf.

37) S. Karheily, A. Moukadem, J.-B. Courbot, and D. Abdeslam, "Time-frequency features for SEMG Signals Classification," Proceedings of the 13th International Joint Conference on Biomedical Engineering Systems and Technologies, 2020. doi:10.5220/0008971902440249.

38) Moses, M. B., Nithya, S. E. & Parameswari, M. (2022). Internet of Things and Geographical Information System based Monitoring and Mapping of Real Time Water Quality System. International Journal of Environmental Sciences, 8(1), 27-36.